にどのように変化するのかに注目しており、2週齢で比が大きくなった要因や関連する受容体については確認するに至っていない。また、2つの刺激の時間間隔は重要である。反回抑制の評価に使われる時間間隔は 5～10 ミリ秒が多い。これは数秒かかるシナプス伝達を 2 回経ているためである。10 秒より長い刺激間隔たとえば20ミリ秒や50ミリ秒くらいになると反回抑制の持続時間すなわち GABA シナプス間隙における GABA の滞在確率を反映すると考えられる。このように、同じ大きさの電気刺激を適当な間隔で 2 回与えるというシンプルな方法で反回抑制が評価できるのである。今回の結果から GABA 系がどのように関与しているのかさらに検討していくための有力は情報を得たと考える。

関野が提示した膜電位感受性色素を用いた評価法には、機器類が高価であること、画像処理方法、定量化などに、まだ解決するべき問題が多数ある。しかし、抑制の広がりに関する空間情報が得られるのは、大変に有益な情報である。

E．結論

本研究で紹介した、抑制性神経回路機能をインビトロ実験で調べる手法は、化学物質の成長期における神経系への影響の評価系として現在利用可能な方法としては簡便な方法である。

動物の行動観察や病理標本により化学物質の中枢神経系に対する影響がこれまでも調べられているが、化学物質の有害反応の発現メカニズムが考慮されていないために、成長期の神経系への有害作用を予測することができなかった。しかし本研究では、有害反応のメカニズムとして、脳の GABA 機能を発達指標として評価しており、生後発達の比較的早い段階で GABA 神経による抑制の発達障害を検出できることが示唆された。

G．研究発表

1．論文発表

なし。

2．学会発表

関野祐子（研究分担者）

[1] 藤枝智美, 三輪秀樹, 白尾智明, 関野祐子, Modulation of neuronal circuits by $GABA_B$ receptor activity in the mouse lateral amygdala（マウス扁桃体外側核の $GABA_B$ 受容体による神経回路機能の修飾）. 神経科学学会 Neuro2011, 横浜, 2011.

[2] 藤枝智美, 三輪秀樹, 白尾智明, 関野祐子, マウス扁桃体外側核の GABA 受容体応答の可塑性に関する研究（Plasticity of GABA receptor activity in the mouse lateral amygdala）. 第 58 回 北関東医学会, 前橋, 2011.

[3] 藤枝智美, 三輪秀樹, 白尾智明, 関野祐子, Inhibitory synaptic plasticity in the mouse lateral amygdala（マウス扁桃体外側核における抑制性シナプス可塑性に関する研究）. 第 2 回 放射線神経生物学研究集会, 前橋, 2011.

吉田祥子（研究協力者）

[1] S. Yoshida , Visualization of GABA release in the developing cerebellar cortex. 8th IBRO World Congress of Neuroscience, Florence, 2011.

[2] M. Tanozaki, N. Hozumi, C. Takayama, A. Fukuda, S. Yoshida, Observation of glutamate and GABA in developing rat cerebellar slices using the enzyme-linked photo assay systems: assay system innovation. AP-IRC, Toyohashi, 2011.

[3] 神部貴仁, 伊藤成希, 穂積直裕, 福田敦夫, 吉田祥子, ラット成熟大脳組織からのグルタミン酸,GABA,ATP 放出を可視化する. 第 34 回神経科学学会,横浜,2011.

[4] A. Fukuda, T. Morishima, T. Kumada, C. Takayama, S. Yoshida, Ambient GABA released from Bergmann glial cells promotes proliferation of cerebellar granule cell precursors. 41th Neuroscience meeting, Washington DC, 2011.

笛田由紀子（研究協力者）

[1] 笛田由紀子, 金光雅成, 夏目季代久, 石田尾徹, 上野晋, 保利一, 海馬シナプスの長期増強に対する 1-ブロモプロパン曝露の影響. 第 84 回日本産業衛生学会, 東京, 2011.

[2] 上野晋, 笛田由紀子, 石田尾徹, 野中美希, 柳原延章, 保利一, フロン代替物質 1-ブロモプロパンの胎生期曝露がおよぼす若年期の記憶機能への影響. 平成 23 年度日本産業衛生学会九州地方学会, 佐賀, 2011.

[3] 笛田由紀子, 上野晋, 石田尾徹, 保利一, フロン代替化学物質 1-ブロモプロパンへの

胎生期曝露は次世代ラットにおいて海馬興奮性のasymmetryを修飾する. 第34回日本神経科学大会, 東京, 2011.

[4] 金光雅成, 笛田由紀子, 江川純恵, 石田尾徹, 上野晋, 保利一, 乳期ラットの行動に対する1-bromopropane胎生期曝露の影響. 平成23年度合同研究会「産業化学物質の神経・行動・発達への影響」, 東京, 2011.

[5] 笛田由紀子, 石田尾徹, 上野晋, 保利一, 胎生期曝露モデル動物の神経生理学的評価による1-ブロモプロパンの次世代に対する中枢神経学的影響の検討. 平成23年度合同研究会「産業化学物質の神経・行動・発達への影響」, 東京, 2011.

[6] 福田留美, 笛田由紀子, 石田尾徹, 由比友顕, 上野晋, 石松維世, 柘野幸生, 樋上光雄, 保利一, 幼若ラットの脳神経発達における1-ブロモプロパン胎児期曝露の影響ーペンチレンテトラゾール感受性と曝露濃度. 第29回産業医科大学学会総会, 北九州, 2011.

H. 知的財産の出願・登録状況

1. 特許出願

吉田祥子（研究協力者）

[1] 生体からのATP、アデノシン、リン酸放出分布可視化デバイス, 吉田祥子, 特願2011-176342 (2011).

2. 実用新案登録

なし。

3. その他

なし。

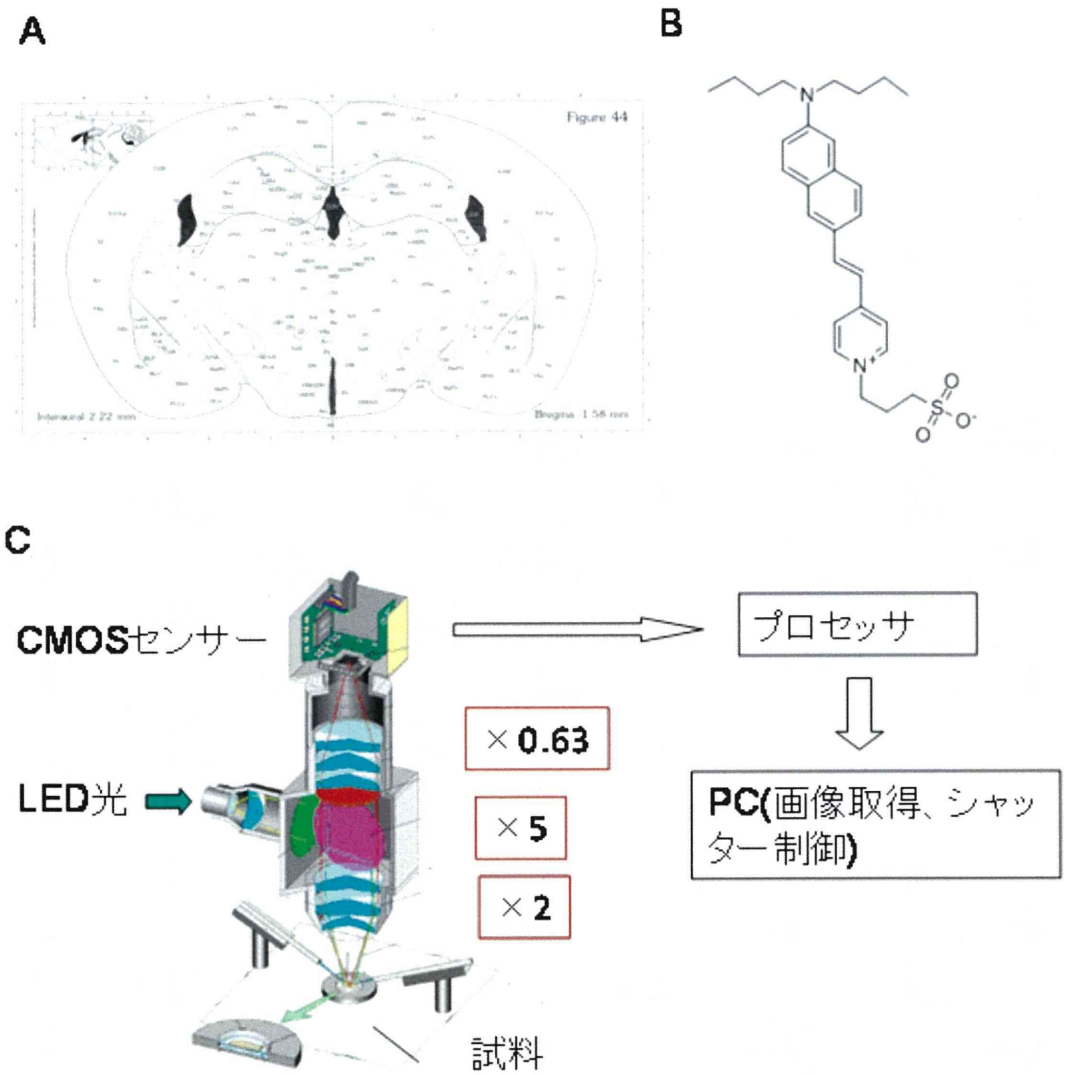

図１．実験方法の概要

A. 扁桃体スライス標本の断面図
マウス脳を摘出し、扁桃体を含む脳部位のブロックから、図の前後付近 400μm のスライス標本を作製した。外包(EC)、扁桃体(LA)、扁桃体基底外側核(BLA)

B. 膜電位感受性色素(Di-4-ANEPPS)

C. 膜電位感受性色素により染色したスライス標本から光学信号を記録する装置
実態顕微鏡のステージの灌流装置にスライスを乗せて、励起光(530±5nm)をあて、蛍光(590～650nm)を上部に取り付けた CMOS センサー(Ultima, Brain Vision Inc. Japan)により、１ミリ秒間隔で画像を撮影した。

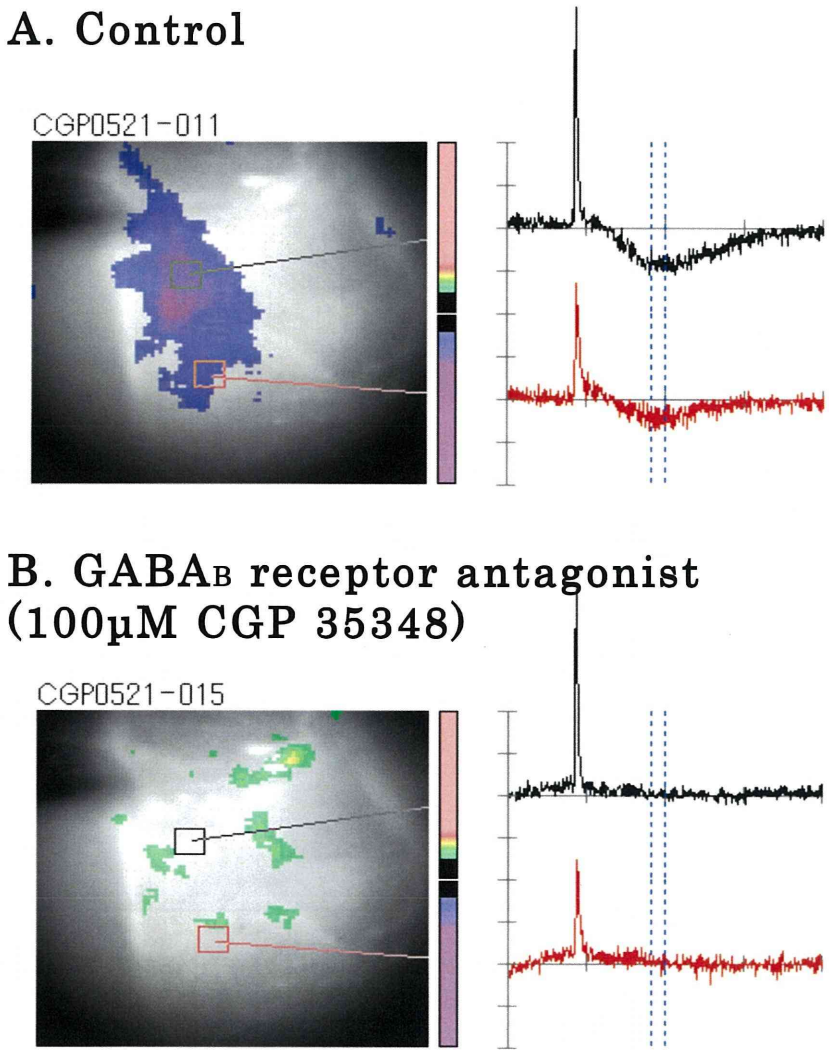

図２．膜電位感受性色素により可視化された GABA による抑制性過分極応答
C. 扁桃体の外側核と基底外側核全体に過分極応答がひろがる様子が可視化された。
D. 刺激後 350 ms 後の画像と黒と赤の四角で示された画像部位の光学応答波形
$GABA_B$ 受容体の阻害薬により遅い過分極成分が消失した。

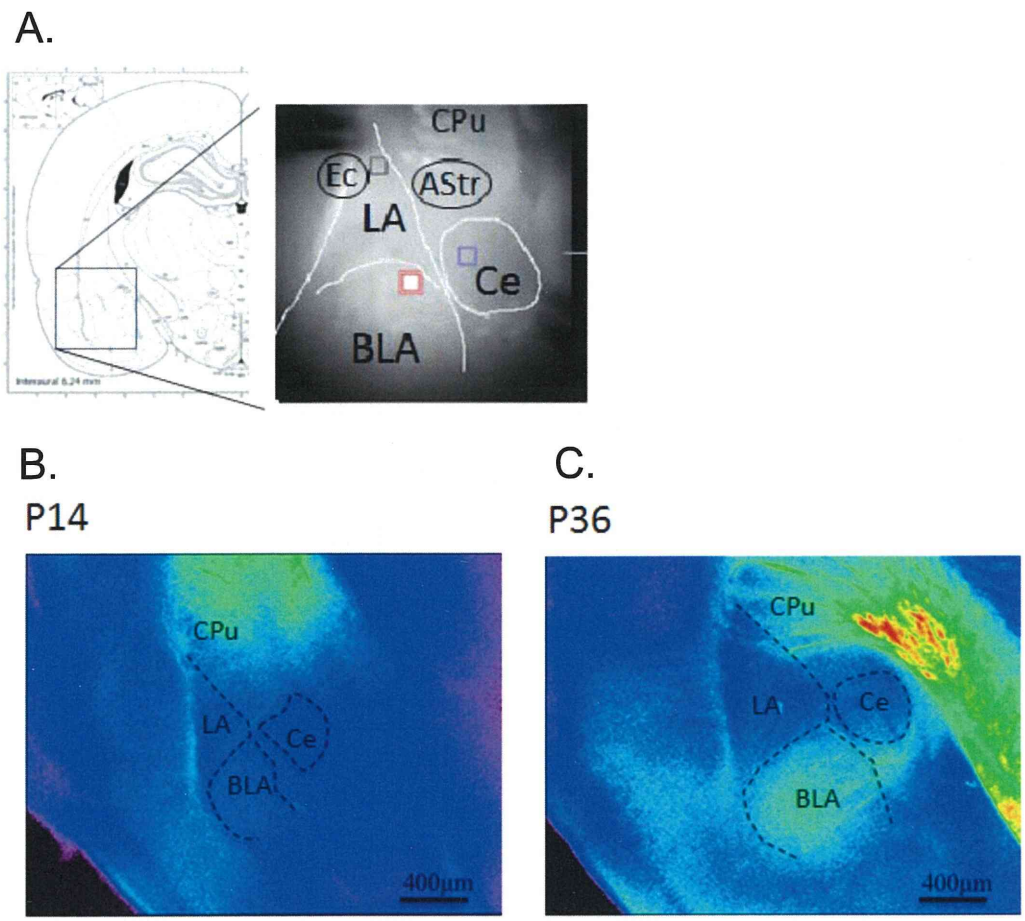

図３．マウス扁桃体スライスからの GABA の自発的遊離の空間分布の可視化
生後 2 週齢と 36 日齢では扁桃体からの GABA 遊離パターンが大きく異なっていた。

A. マウス脳の扁桃体部位を示す脳定位マップとスライスの部位を示した図
外側核（LA）、基底外側核（BLA）、中心核（Ce）、外包（EC）、扁桃体線条体移行部（AStr）、線条体（CPu）。青が遊離の低いところ、遊離が多くなるほど、緑から黄色、赤と疑似カラーで表示している。

B. 生後 14 日のマウス扁桃体スライスからの GABA 遊離。扁桃体からの遊離は少ない。Cpu には GABA の遊離が見られる。

C. 生後 36 日のマウス扁桃体スライスからの GABA 遊離。扁桃体内では BLA に限定して遊離量がふえている。線条体で高い遊離量が認められた。

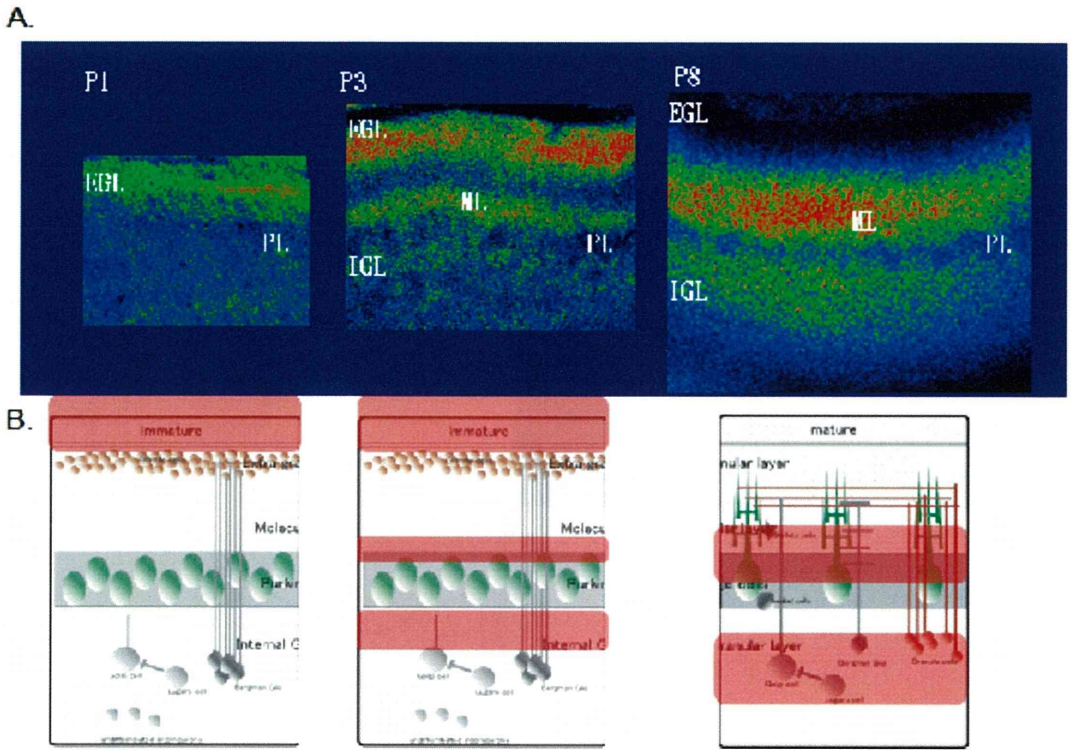

図４．マウス小脳スライスからの GABA の自発的遊離の空間分布の可視化
Ａ．生後１日、３日、８日と、成長するにつれて小脳の細胞層での GABA 遊離のパターンが大きく変化していく様子。
Ｂ．小脳の成長期の細胞層の模式図と、GABA の遊離が多い部位を赤で表現した模式図である。

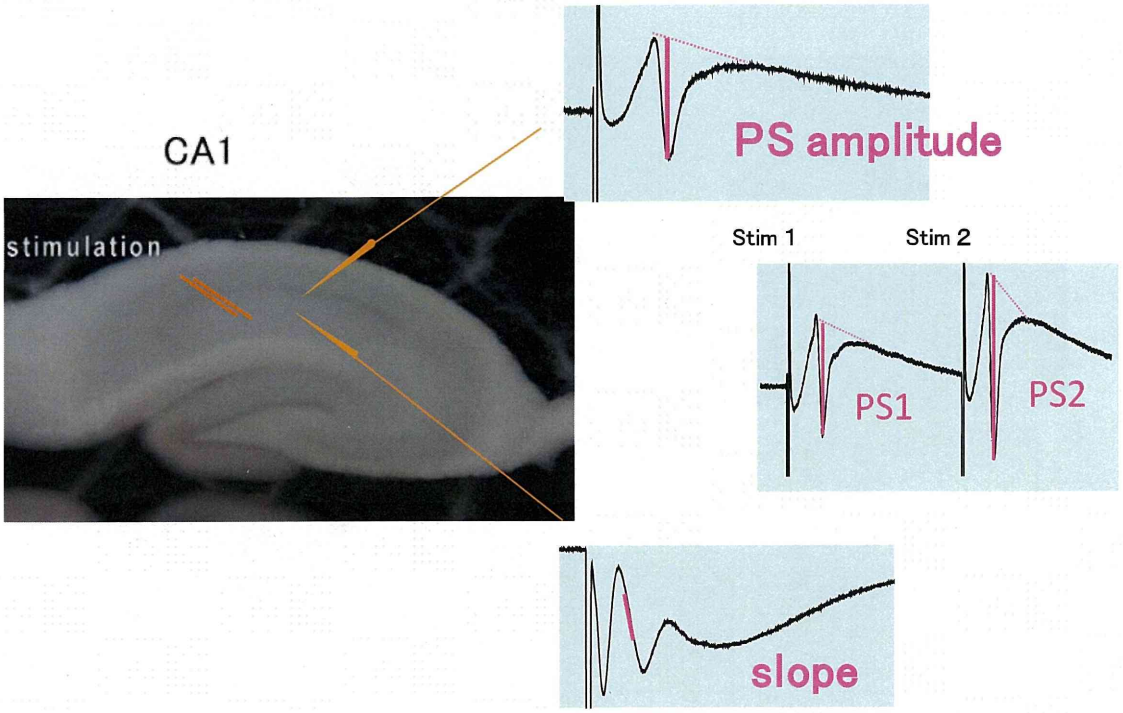

図５．実体顕微鏡下で観察される海馬スライス標本と神経細胞の応答

左の写真は海馬スライス標本である。CA1 領野シナプス層に挿入された 2 本の線は刺激電極を表している。CA1 領野に書かれた 2 本の矢印は記録電極を表す。記録は錐体細胞層とシナプス層からされた。神経細胞の応答は 2 週齢のラットから記録されたものである。上の応答は細胞層から記録されたもので集合スパイク電位が記録されている。集合スパイク電位の振幅の大きさを PS amplitude と定義した。PS amplitude の大きさは、ナトリウムイオンの流入による活動電位を発生した神経細胞の数を反映ものである。下の応答はシナプス層から記録されたもので集合シナプス後電位が記録されている。太線で示された部分はシナプス電位が大きくなるようすを定量的に示すもので slope と定義した。Slope は AMPA 型グルタミン酸受容体の活性化の大きさ、すなわち興奮性シナプスの活性化の大きさを表す。真ん中の応答は、ダブルパルスへの応答を示す。1 回目の電気刺激への応答を PS1、2 回目の電気刺激に対して得られた応答を PS2 として、PS amplitude2/PS amplitude1 の比を計算した。シナプス電位の slope についても、図には示されていないが、slope2/slope1 の比を計算した。

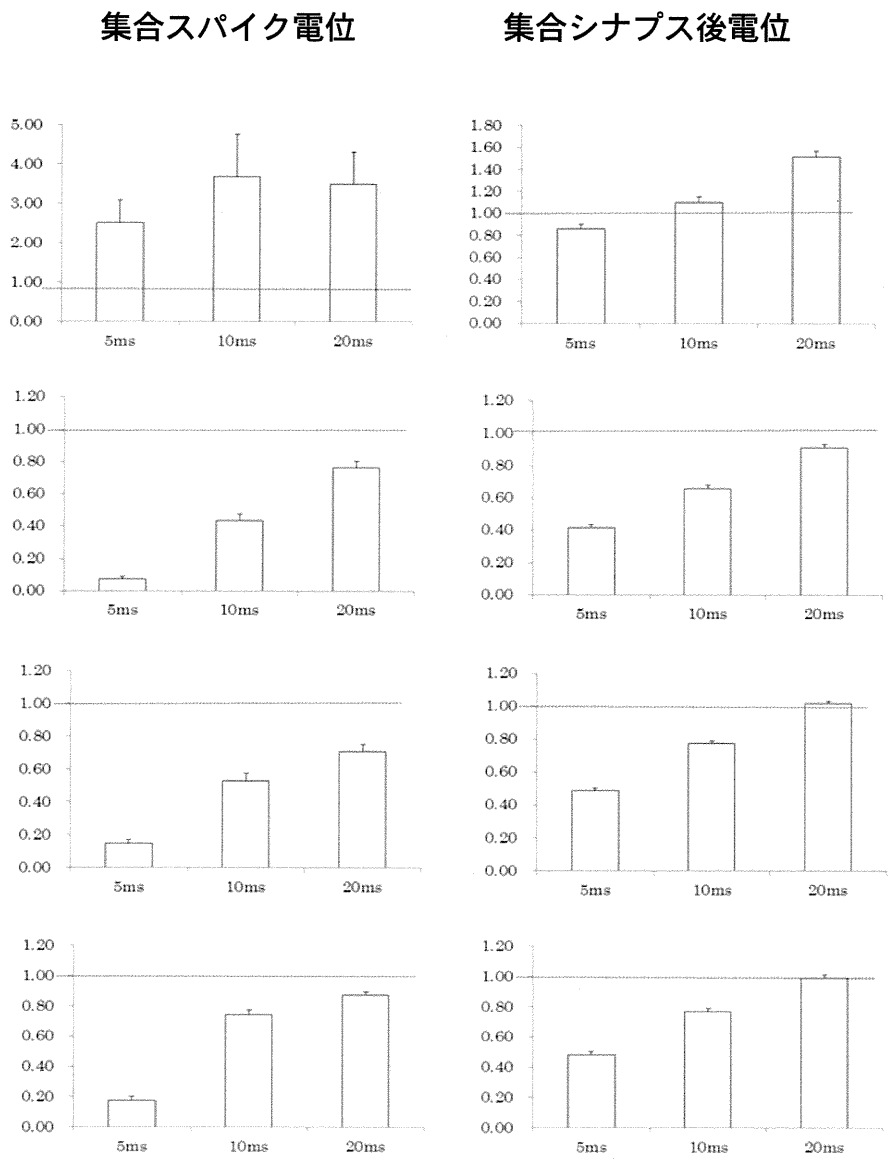

図６．ラットの脳の発達と海馬 CA1 領域のペアパルス比
左の 4 枚のグラフは細胞層から記録された集合スパイク電位の振幅(PS amplitude)の比を刺激間隔ごとに計算したものである。右の 4 枚のグラフはシナプス層から記録されたシナプス後電位の傾き(slope)の比を刺激間隔ごとに計算したものである。ラットの週齢は、上から 2 週齢、5 週齢、8 週齢、13 週齢である。点線は比が 1 であることを示した。

研究成果の刊行に関する一覧表

雑誌

発表者氏名	論文タイトル名	発表誌名	巻号	ページ	出版年
M. Tanaka, T. Nagai, M. Usami, K. Hasui, S. Takao, T. Matsuyama	Phenotypic and functional profiles of CRIg (Z39Ig)-expressing macrophages in the large intestine.	Innate Immunity	18	258-267	2012
K. Sato, J. Kuriwaki, K. Takahashi , Y. Saito, J. Oka, Y. Otani, Y. Sha, K. Nakazawa, Y. Sekino, T. Ohwada	Discovery of a tamoxifen-related compound that suppresses glial L-glutamate transport activity without Interaction with estrogen receptors.	ACS Chem Neurosci	3	105-113	2013
F. Takata, S. Dohgu, A. Yamauchi, J. Matsumoto, T. Machida, K. Fujishita, K. Shibata, Y. Shinozaki, K. Sato, Y. Kataoka, S. Koizumi	In vitro blood-brain barrier models using brain capillary endothelial cells isolated from infant and adult rats retain age-related barrier properties.	Plos ONE			印刷中
Y. Morizawa, K. Sato, J. Takaki, A. Kawasaki, K. Shibata, T. Suzuki, S. Ohta, S. Koizumi	Cell-autonomous enhancement of glutamate-uptake by female astrocytes.	Cell Mol Neurobiol			印刷中
佐藤　薫	グリア型グルタミン酸トランスポーター	日薬理誌	138	127	2011
Y. Kanda, T. Hinata, S.W. Kang S.W., Y. Watanabe	Reactive oxygen species mediate adipocyte differentiation in mesenchymal stem cells.	Life Sciences	89	250-258	印刷中
W. Lin, N. Hirata, Y. Sekino, Y. Kanda	Role of α7-Nicotinic Acetylcholine Receptor in Normal and Cancer Stem Cells.	Current Drug Targets			印刷中
R. Kikura-Hanajiri, M. Kawamura, A. Miyajima, M. Sunouchi, Y. Goda	Chiral analyses of dextromethorphan/levomethorphan and their metabolites in rat and human samples using LC-MS/MS.	Anal Bioanal Chem	400	153-155	2011
簾内桃子	トキシコキネティクス, 代謝試験の実験手法.	最新　動物実験代替法の技法ノウハウ		262-270	2011

研究成果の刊行物・別刷

ACS Chemical Neuroscience

Research Article

pubs.acs.org/acschemicalneuroscience

Discovery of a Tamoxifen-Related Compound that Suppresses Glial L-Glutamate Transport Activity without Interaction with Estrogen Receptors

Kaoru Sato,*[,‡,†] Jun-ichi Kuriwaki,[‡,†] Kanako Takahashi,[‡] Yoshihiko Saito,[§] Jun-ichiro Oka,[§] Yuko Otani,[∥] Yu Sha,[∥] Ken Nakazawa,[‡] Yuko Sekino,[‡] and Tomohiko Ohwada*[,∥]

[‡]Laboratory of Neuropharmacology, Division of Pharmacology, National Institute of Health Sciences, 1-18-1 Kamiyoga, Setagaya-ku, Tokyo 158-8501, Japan

[§]Laboratory of Pharmacology, Faculty of Pharmaceutical Sciences, Tokyo University of Science, 2541 Yamazaki, Noda-city, Chiba 278-8510, Japan

[∥]Laboratory of Organic and Medicinal Chemistry, Graduate School of Pharmaceutical Sciences, University of Tokyo, 7-3-1, Hongo, Bunkyo-ku, Tokyo 113-0033, Japan

ABSTRACT: We recently found that tamoxifen suppresses L-glutamate transport activity of cultured astrocytes. Here, in an attempt to separate the L-glutamate transporter-inhibitory activity from the estrogen receptor-mediated genomic effects, we synthesized several compounds structurally related to tamoxifen. Among them, we identified two compounds, **1** (YAK01) and **3** (YAK037), which potently inhibited L-glutamate transporter activity. The inhibitory effect of **1** was found to be mediated through estrogen receptors and the mitogen-activated protein kinase (MAPK)/phosphatidylinositol 3-kinase (PI3K) pathway, though **1** showed greatly reduced transactivation activity compared with that of 17β-estradiol. On the other hand, compound **3** exerted its inhibitory effect through an estrogen receptor-independent and MAPK-independent, but PI3K-dependent pathway, and showed no transactivation activity. Compound **3** may represent a new platform for developing novel L-glutamate transporter inhibitors with higher brain transfer rates and reduced adverse effects.

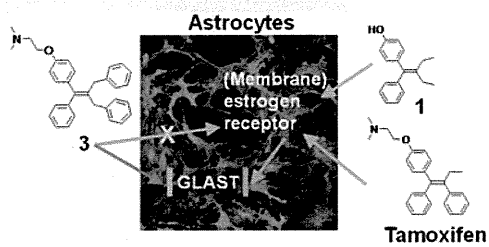

Inhibition of glial L-glutamate transporter

KEYWORDS: *Tamoxifen, astrocyte, L-glutamate transporter, ERα, tetrasubstituted ethylene, nongenomic pathway*

L-Glutamate (L-Glu) is one of the major excitatory neurotransmitters in the central nervous system (CNS), but high concentrations of extracellular L-Glu cause excessive stimulation of L-Glu receptors in the CNS, leading to neurotoxicity.[1,2] Astrocyte L-Glu transporters are the only machinery available to remove L-Glu from extracellular fluid and to maintain a low and nontoxic concentration of L-Glu.[3] Consequently, dysfunction of astrocyte L-Glu transporters is considered to be implicated in the pathology of neurodegenerative conditions.[4] Therefore, exogenous compounds that can regulate the function of L-Glu transporters may provide chemical tools to investigate the regulatory mechanisms of these transporters at the molecular level, and would also be candidate therapeutic agents.

There is growing evidence that estrogen receptor (ER) α, which is a nuclear ER (nER) that mediates genomic effects, can also be translocated to plasma membranes and mediate acute nongenomic effects in some cases. We have clarified that 17β-estradiol (E2) inhibits L-Glu transporters via a nongenomic pathway involving membrane-associated ERα (mERα).[5] Tamoxifen (Tam), a synthetic estrogen analogue that is clinically used in the treatment of breast cancer to block the proliferative action of estrogens,[6] also inhibited astrocyte L-Glu transporters at picomolar concentration, probably through the same nongenomic pathway as E2.[7] Because overexpression of astrocyte L-Glu transporters is often associated with neuropsychiatric disorders,[4] inhibitors of L-Glu transporters may be clinically useful to ameliorate these disorders.[8] However, Tam also acts on genomic pathways involving nuclear estrogen receptors (nERs) α and β, depending on the cell type and promoter context,[9] and so may cause adverse effects including endometrial changes, depression and weight gain.[10,11] Therefore, Tam-inspired compounds that retain the inhibitory effect on L-Glu transporters, but lack the nER-mediated genomic effects, would be useful tools for biological research, as well as candidate therapeutic agents.

Tam is a tetrasubstituted triphenylethylene derivative, in which the four substituents on the olefinic carbon atoms are different. This structural complexity makes the stereospecific synthesis of Tam-related derivatives difficult. We thus focused on Tam-inspired compounds bearing identical substituents on at least one of the olefinic carbon atoms.[12] It is well-known that the *N,N*-dimethylaminoethyl substituent on the phenolic oxygen atom and the regiochemistry of the tetrasubstituted

Received: September 29, 2011
Accepted: November 14, 2011
Published: November 14, 2011

olefin of Tam are crucial for ER binding activity.[13] So, we considered that more symmetrical derivatives of Tam might show reduced ER-binding ability.

Among our synthesized compounds, we found two, compounds **1** (YAK01) and **3** (YAK037), with potent L-Glu transporter-inhibitory activity. Studies of their mechanisms of action indicated that, unlike Tam, compound **3** acts through an ER-independent and MAPK-independent, but PI3K-dependent pathway and shows no transactivation activity for nERs. We believe this compound may represent a new platform for developing novel L-Glu transporter inhibitors with higher brain transfer rates and reduced adverse effects.

RESULTS AND DISCUSSION

We synthesized several Tam-inspired compounds bearing identical substituents on one carbon atom of the olefin,[12] and found that two of them were potent inhibitors of astrocyte L-Glu transporters. The diethyl-substituted derivative **1** inhibited L-Glu transporters in the picomolar range (62.7 ± 7.48% of control at 1 pM; Figure 2A). The dose–response curve for the inhibitory activity was not linear, but followed an inverted U-shaped curve; however, such a non-monotonic dose dependence is rather common for hormones and their mimetics.[14] On the other hand, when the symmetrical substituent was changed from ethyl to benzyl (**2**), the inhibitory effect was lost (Figure 2B). However, when the phenolic oxygen atom of **1** was substituted with a *N,N*-dimethylaminoethyl group (Figure 1C), we found

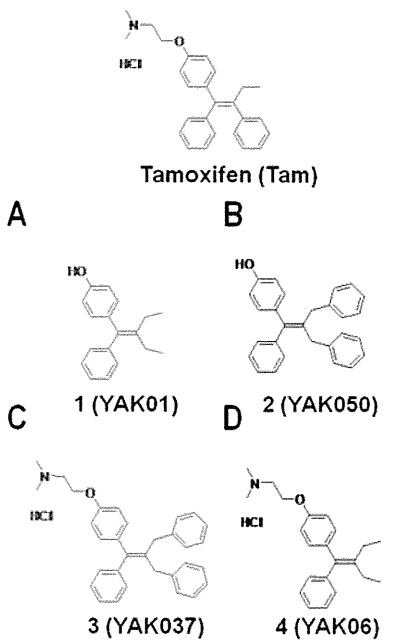

Figure 1. Chemical structures of the newly synthesized tamoxifen-related compounds.

that the resulting compound **3** showed dose-dependent L-Glu transporter inhibition in the picomolar range (63.8 ± 5.49% of control at 1 pM; Figure 2C). The dose-dependency of the effect of **3** suggested that the underlying mechanism might be different from that in the case of **1**. Compound **4** was inactive (Figure 2D).

We next examined the effects of **1** and **3** on cell viability by means of MTT reduction assay and LDH leakage assay, using the same cultured sample. Neither of the compounds was cytotoxic at concentrations below 1 μM (Figure 3), though 100 μM **1** and 10 μM **3** caused severe cell damage. These results exclude the possibility that the L-Glu clearance-inhibitory effects of these compounds at concentrations below 1 μM were caused by cell damage.

In order to confirm the involvement of L-Glu transporters in the inhibition of L-Glu uptake by our compounds, and to rule out the possibility that **1** and **3** act by inducing L-Glu release from astrocytes, we next examined the effect of **1** and **3** on L-Glu clearance when the L-Glu transporter activity was blocked with TBOA, a potent nonselective L-Glu transporter inhibitor (IC_{50}: 48 μM for GLAST/EAAT1, 7 μM for GLT1/EAAT2). We confirmed that application of 1 mM TBOA potently inhibited L-Glu transporter activity; that is, TBOA caused reversible chemical knock-down of L-Glu transporter activity.[7] When either **1** or **3** was coapplied with 1 mM TBOA, these compounds no longer influenced L-Glu clearance (Figure 4), indicating that the actions of these compounds are indeed mediated by L-Glu transporters, and do not involve L-Glu release from astrocytes.

Our cultured astrocytes predominantly expressed ERα, and little or no expression of ERβ was detected.[5] Tam is known to be a partial agonist of ERs,[9] raising the possibility that the compounds exerted their inhibitory effects via interaction with ERα. Therefore, we examined the involvement of ERα by coapplication of ICI182,780, a high-affinity antagonist of ERs. ICI182,780 dose-dependently blocked the inhibition of L-Glu uptake caused by **1** (Figure 5A) at 0.01, 0.1, and 1 μM, at which the effects of Tam were reported to be completely suppressed.[7] In contrast, ICI182,780 had no effect on the inhibition by **3** (Figure 5B), suggesting that the mechanism of the inhibition by **3** is independent of ERs. We further examined the signal transduction pathways mediating the effects of **1** and **3**. When coapplied with U0126, which inhibits mitogen-activated protein kinase/extracellular signal-regulated kinase 1 (MEK1, IC50: 70 nM) and MEK2 (IC50: 60 nM), the inhibitory effect by **1** was blocked, whereas that of **3** was not (Figure 6A). On the other hand, when coapplied with LY294002, a specific phosphoinositide 3-kinase (PI3K) inhibitor (IC50: 70 nM), the inhibitory effects of both compounds were completely blocked (Figure 6B). These results suggest that PI3K is a common mediator of the effects of both compounds, whereas mitogen-activated protein kinase (MAPK) is involved only in the mechanism of inhibition by **1**.

Finally we examined the ER-agonist potency of **1** and **3**, i.e., the transcriptional effects of these compounds via human ERα and ERβ, using HEK293/hERα and HEK293/hERβ reporter cells (Figure 7). Compound **1** showed agonist activity in both of 293/hERα and 293/hERβ reporter cells, though the binding affinities were much weaker than that of E2. The EC50 values of **1** for ERα and ERβ are 30.8 nM and 10.4 nM, respectively (1.25 nM and 0.864 nM, respectively, for E2). The relative agonist activity of **1** was 66.8% of that of E2 in HEK293/hERα and 122.0% of that of E2 in HEK293/hERβ. Strikingly, **3** showed no agonist potency for ERα or ERβ. These findings strongly suggest that **3** can inhibit L-Glu transporters without interaction with ERs.

In this study, we examined the potential of Tam-related compounds to inhibit GLAST/EAAT1 and GLT1/EAAT2, which are major astrocytic L-Glu transporters in the rat

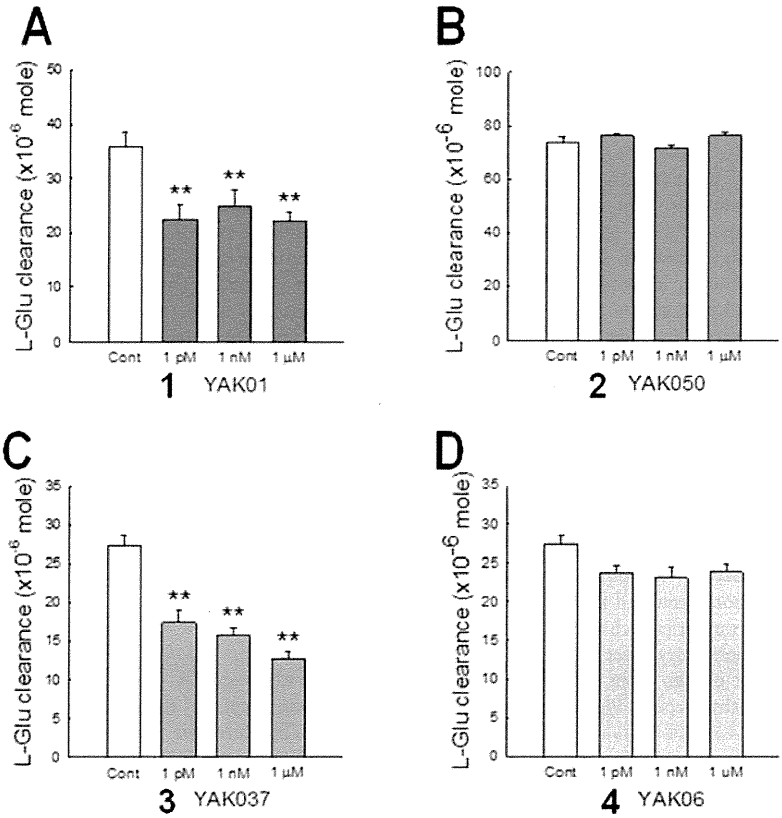

Figure 2. Compounds **1** and **3** inhibited L-Glu clearance in cultured astrocytes. The open column shows the control clearance, and colored columns show the clearance in the presence of various concentrations of compounds **1** (A), **2** (B), **3** (C), and **4** (D). $^{**}p < 0.01$ vs control group ($N = 6$), Tukey's test following ANOVA.

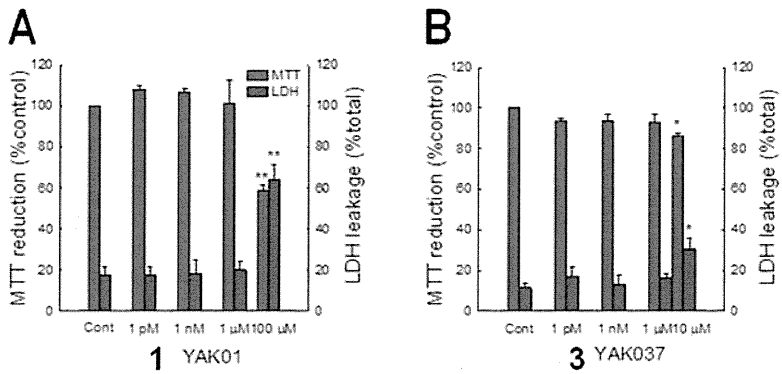

Figure 3. Effects of compounds **1** and **3** on cell viability. The results of MTT reduction and LDH leakage assays of **1** (A) and **3** (B) are shown. $^{*}p < 0.05$, $^{**}p < 0.01$ vs control group ($N = 6$), Tukey's test following ANOVA.

forebrain. Although GLT-1 is the main regulator of synaptically released L-Glu in vivo, the predominant subtype changes to GLAST in cultured astrocytes, possibly owing to the lack of interaction of astrocytes with neurons.[15] We confirmed that GLAST is the main functional L-Glu transporter in our primary-cultured astrocytes by Western blotting and pharmacological experiments (data not shown), in accordance with a previous report.[16] Therefore, the effects of the compounds observed here can be interpreted as being due to modulation of GLAST functional activity.

There is growing evidence that ERα, which is a nER that mediates genomic effects, can also be translocated to plasma membranes and mediate acute nongenomic effects in some cases. Transfection of CHO cells with nERs was reported to result in ER expression in both nuclei and membranes.[17] ERs on the plasma membranes of tumor cells were demonstrated to be structurally similar to nERs.[18] Further, mERα activated metabotropic glutamate receptor 5 (mGluR5) in striatal neurons in the CNS.[19] In our previous study, we clarified that the predominant ER subtype in cultured astrocytes was ERα, and

dx.doi.org/10.1021/cn200091w | ACS Chem. Neurosci. 2012, 3, 105–113

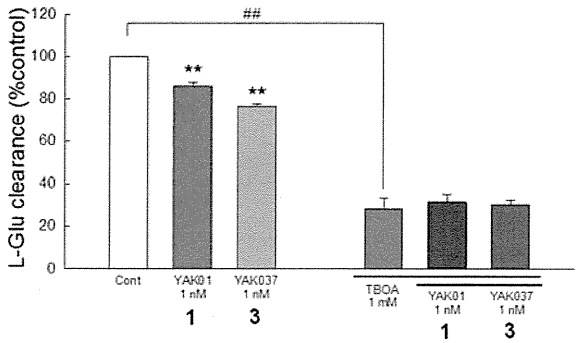

Figure 4. Compounds **1** and **3** suppressed L-Glu clearance in astrocyte culture by decreasing the functional activity of L-Glu transporter. L-Glu clearance in the presence and absence of compounds **1** and **3** is shown, together with their effects in the copresence of the potent nonselective L-Glu transporter inhibitor TBOA. $^{**}p < 0.01$ vs control group ($N = 6$), Tukey's test following ANOVA.

estrogens (such as E2 and Tam) inhibited L-Glu transporter activity via the activation of mERα.[5] We found that the effects of **1** were blocked by ICI182,780, suggesting an interaction of **1** with ERα. In addition, our pharmacological experiments showed that activation of both of MAPK and PI3K is necessary for the L-Glu transporter-inhibitory activity of **1**. There are many reports indicating that nongenomic effects involving mERα are mediated via MAPK[19−21] and PI3K.[20,22] Taken together, the effects of **1** may be mediated by mERα in a similar manner to E2 and Tam. E2 was reported to activate MAPK via both PI3K-dependent and independent pathways in a single neuron.[20] Whether or not the same signaling pathways also exist in astrocytes is not yet known. It is of interest that other studies have found that estrogens also inhibit dopamine transporter (DAT) through the activation of mERα.[23,24]

On the other hand, the effect of **3** was ER-independent and MAPK-independent, but PI3K-dependent. Our binding assay revealed that **1** binds with ERs, but **3** does not. Based on these results, we propose that the mechanisms of the L-Glu

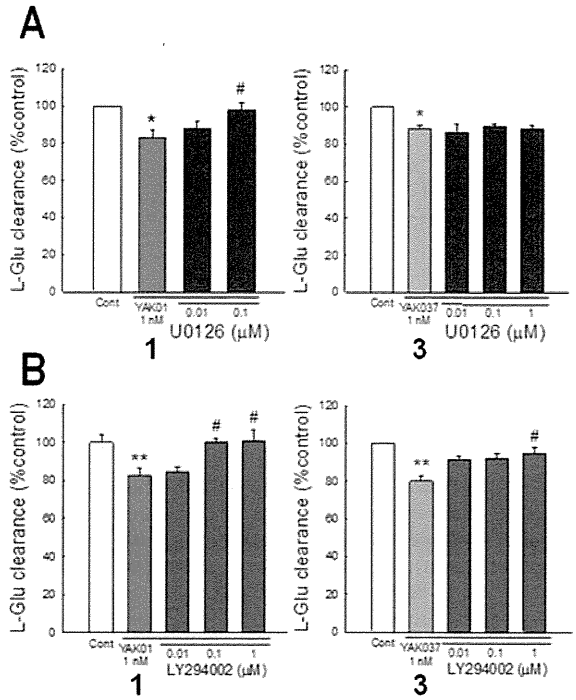

Figure 6. Involvement of MAPK and PI3K in the L-Glu transporter-inhibitory activity of compounds **1** (A) and **3** (B). Effects of compounds **1** (left panels) and **3** (right panels) on L-Glu clearance in the presence and absence of various concentrations of U0126, an inhibitor of MAPK/ERKs (A) or LY294002, a specific inhibitor of PI3K (B). $^{*}P < 0.05$, $^{**}p < 0.01$ vs control group, $\#p < 0.05$ vs compound-treated group ($N = 6$), Tukey's test following ANOVA.

transporter-inhibitory effects of **1** and **3** are different, as illustrated in Figure 8. The effect of **3** was possibly mediated by GPR30, a newly found ER, which is suggested to mediate the rapid nongenomic effects of estrogens.[25,26] In the case of GPR30, ICI182,780 acts as agonist, leading to activation of

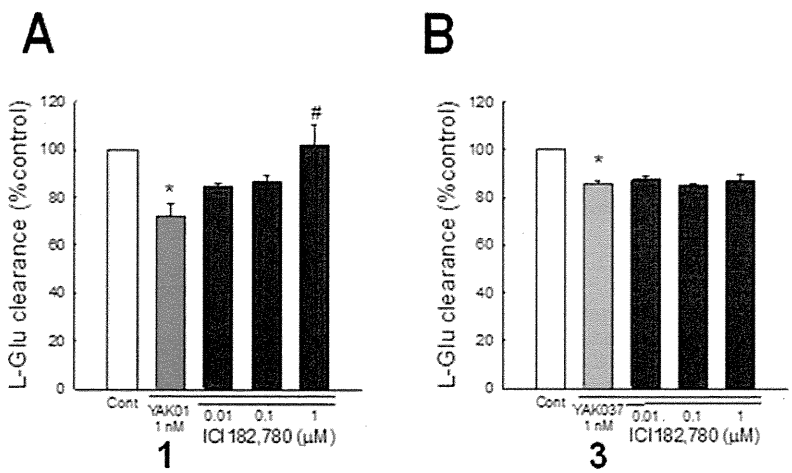

Figure 5. Involvement of ERs in the L-Glu transporter-inhibitory effects of compounds **1** and **3**. Effects of compounds **1** (A) and **3** (B) on L-Glu clearance in the presence and absence of various concentrations of ICI182,780, a high-affinity antagonist of ERs. $^{*}P < 0.05$ vs control group, $\#p < 0.05$ vs compound-treated group ($N = 6$), Tukey's test following ANOVA.

dx.doi.org/10.1021/cn200091w | ACS Chem. Neurosci. 2012, 3, 105–113

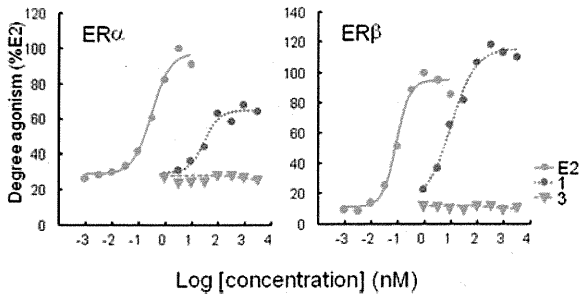

Figure 7. ER agonist potency of compounds **1** and **3** to nERs: dose dependence of binding of compounds **1** and **3** in HEK293/hERα cells (left) or HEK293/hERβ cells (right). Compound 1 showed dose-dependent agonist activity in both of HEK293/hERα cells (left) and HEK293/hERβ cells (right), though 3 showed no agonist potency for ERα or ERβ.

signal transduction pathways in a similar manner to estrogens.[27,28] However, we could not detect any effects of ICI182,780 alone on L-Glu transporter in our experiments (data not shown). In addition, Kuo et al. reported that GPR30 in astrocytes is detected not in the cell membranes but in the smooth endoplasmic reticulum,[29] while the cellular localization of GPR30 has been still controversially argued. In these contexts, GPR30 is an unlikely mediator to block the L-Glu transporters by the action of **3**.

According to Kisanga et al., the concentration of Tam in serum during conventional treatment for breast cancer (1–20 mg daily) is in the range from 20 to 225 nM.[30] Because **3** is more hydrophobic than Tam (the values of clogP for Tam and **3** are 7.56 and 9.70, respectively), it should exhibit greater permeability into the brain. Although other L-Glu transporter inhibitors, mainly L-Glu/aspartate analogues, are known, few of them have high brain transfer rates. Therefore, **3** is expected to be useful for biological research, and is also considered to be a promising candidate or lead compound for pharmacological application.

In conclusion, examination of several Tam-inspired compounds led to the discovery of two compounds that inhibited astrocytic L-Glu transporters at picomolar concentration. The inhibitory activity of compound **1** was mediated through the ER-MAPK/PI3K pathway, like that of Tam, though its transactivation activity was drastically reduced as compared with E2. In contrast, the inhibitory effect of **3** was manifested through an ER-independent and MAPK-independent, but PI3K-dependent pathway, and **3** showed no transactivation activity. These results suggest that **3** may represent a new platform for the development of novel L-Glu transporter inhibitors with higher brain transfer rates and reduced adverse effects.

■ METHODS

Chemistry. *General Procedures.* All reagents were commercial products and were used without further purification, unless otherwise noted. NMR data were recorded on a JEOL-400 or a Bruker Avance 400 NMR spectrometer (400 MHz for ^{1}H NMR and 100 MHz for ^{13}C NMR). *d*-$CDCl_3$ was used as a solvent, unless otherwise noted. Chemical shifts (δ) are reported in ppm with respect to internal tetramethylsilane (δ = 0 ppm) or undeuterated residual solvent (i.e., $CHCl_3$ (δ = 7.265 ppm)). Coupling constants are given in hertz. Coupling patterns are indicated as follows: m = multiplet, d = doublet, s = singlet, br = broad. High-resolution mass spectrometry (HRMS) was conducted in the electron spray ionization (ESI)-time-of-flight

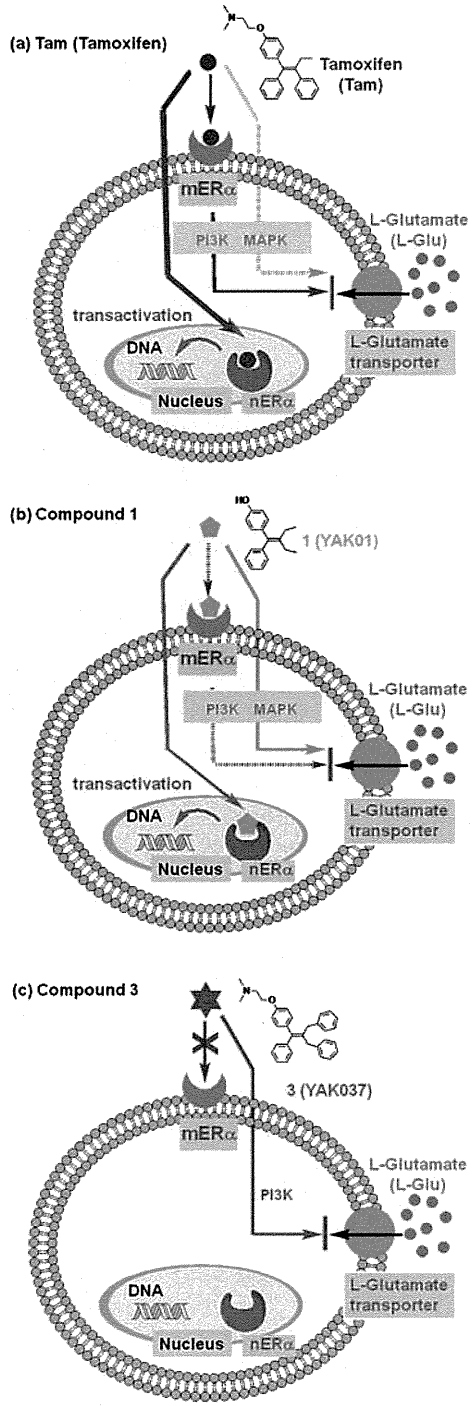

Figure 8. Schematic illustration of the proposed mechanisms of the effects of tamoxifen (a) and compounds **1** (b) and **3** (c).

(TOF) detection mode on a Bruker micrOTOF-05. FAB-MS and high-resolution FAB-MS were obtained on a JMS700-MSTATION (JEOL, Japan). Column chromatography was carried out on silica gel (silica gel 60N (100–210 μm), Kanto Chemicals, Japan). Flash column chromatography was performed on silica gel H (Merck, Germany). Analytical thin-layer chromatography (TLC) was performed on

precoated plates of silica gel HF_{254} (Merck, Germany). All the melting points were measured with a Yanaco Micro Melting Point apparatus and are uncorrected. Combustion analyses were carried out in the microanalysis laboratory of this faculty.

Synthesis of Compounds. Compounds **1** and **2** were synthesized from 4-hydroxybenzophenone and butyl-3-one or dibenzylacetone by using $TiCl_4$ in the presence of Zn. Introduction of the *N,N*-dimethylaminoethyl moiety at the phenolic hydroxyl group of **1** and **2** was carried out by base treatment, followed by addition of 2-dimethylaminoethyl chloride hydrochloride.

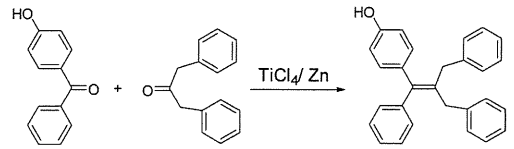

2 (YAK050)

*Synthesis of Tamoxifen-Related Compounds. Compound **2** (YAK050).* To a suspension of Zn powder (916.6 mg; 6.9 equiv with respect to 4-hydroxybenzophenone) in dry THF (30 mL) in a 200 mL three-necked flask, $TiCl_4$ (0.61 mL, 2.8 equiv) was added dropwise under an argon atmosphere at −20 °C (in an ice-salt bath) over 2 min. The resulting light green-yellow mixture was stirred at −20 °C for 20 min and then the cooling bath was removed. After 20 min, the flask was immersed in a preheated oil bath at 100 °C and refluxed at 100 °C with stirring for 2.5 h. To the resulting deep blue mixture was added in one portion a solution of 4-hydroxybenzophenone (401.3 mg, 2.02 mmol) and dibenzyl ketone (1.2735 g, 3 equiv) in 50 mL of dry THF. The resultant mixture was heated at reflux at 100 °C with stirring for 2 h, then allowed to cool to rt, and poured into 400 mL of 0.5 N aqueous NaOH solution. The whole was extracted with ethyl acetate (500 mL). The organic layer was washed with water, dried over $MgSO_4$ and evaporated to give a pale yellow oil (1.5172 g), which was column-chromatographed (silica gel, acetone/*n*-hexane (1:7)) to give 365.0 mg (48% yield) of the olefin **2** as a white amorphous solid. Mp: 57–60 °C. ^{1}H NMR ($CDCl_3$): δ: 7.287–7.079 (m, 17H), 6.760 (d, 2H, J = 8.8 Hz), 4.792 (s, 1H), 3.413 (s, 2H), 3.377 (s, 2H). ^{13}C NMR ($CDCl_3$): δ: 154.1, 143.0, 140.7, 140.4, 135.8, 135.4, 130.7, 129.4, 128.8, 128.3, 128.3, 128.2, 126.5, 125.9, 115.1, 37.4, 37.2. HRMS (ESI^-): Calcd. for $C_{28}H_{23}O$ ($[M - H]^-$), 375.1754. Found: 375.1744. Anal. Calcd for $C_{28}H_{24}O \cdot 0.2H_2O$: C, 88.48; H, 6.47; N, 0.00. Found: C, 88.36; H, 6.63; N, 0.00.

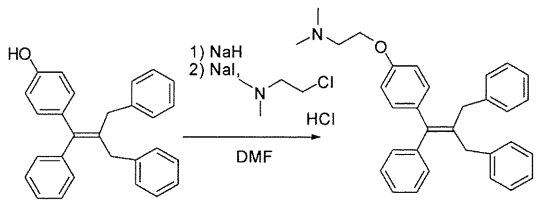

2 (YAK050)

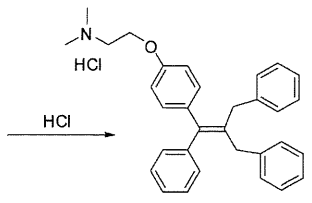

3 (YAK037)

*Compound **3** (YAK037).* To a suspension of NaH (60%, 42 mg, 1.05 mmol) in DMF (3 mL) at 0 °C was added a solution of the phenol **2** (158.2 mg, 0.420 mmol) in DMF (3 mL). The reaction mixture was stirred for 30 min at 0 °C, and then a solution of 2-dimethylaminoethyl chloride hydrochloride (181.0 mg, 1.256 mmol, 3.0 equiv) and NaI (94.0 mg, 0.627 mmol, 1.5 equiv) in DMF (3 mL) was added. The reaction mixture was stirred at 50 °C for 30 min, and then saturated aqueous NH_4Cl was added to quench the reaction. The mixture was extracted with Et_2O. The organic layer was washed with brine, dried over Na_2SO_4 and evaporated to afford a residue, which was column-chromatographed (ethyl acetate/Et_3N = 100/1) to give the intermediate amine (83.0 mg, 44% yield). The HCl salt of the resultant amine was prepared by repeated addition of a solution of 2 N HCl in Et_2O to a solution of the amine in ethyl acetate, followed by evaporation of the organic solvent to give **3**.

3: White solid. Mp. 169–170 °C. ^{1}H NMR ($CDCl_3$): δ: 13.073 (brs, 1H), 7.306–7.195 (m, 13H), 7.102–7.074 (m, 4H), 6.832 (d, 2H, J = 8.8 Hz), 4.481–4.459 (m, 2H), 3.425–3.390 (m, 6H), 2.893 (s, 6H). ^{13}C NMR ($CDCl_3$) δ: 155.7, 142.8, 140.4, 140.3, 140.2, 136.8, 136.2, 130.9, 129.4, 128.8, 128.7, 128.4, 128.3, 128.3, 126.6, 126.0, 125.9, 114.3, 62.8, 56.5, 43.6, 37.4, 37.2. HRMS (ESI^+, $[M + H]^+$): Calcd. for $C_{32}H_{34}NO$, 448.26349. Found: 448.26092. Anal. Calcd for $C_{32}H_{34}ClNO \cdot 1/4H_2O$: C, 78.67; H, 7.12; N, 2.87. Found: C, 78.64; H, 7.30; N, 2.87.

*Compound **1** (YAK01).*

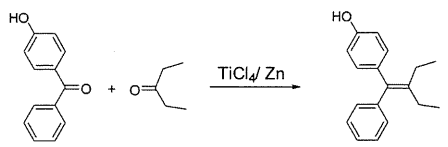

1 (YAK01)

To a suspension of Zn (0.86 g, 13.2 mmol) in 30 mL of dry THF at −5 °C was added dropwise $TiCl_4$ (0.72 mL, 6.6 mmol) under an argon atmosphere. The mixture was heated at reflux for 2 h. A solution of 4-hydroxybenzophenone (341.1 mg, 1.7 mmol) and 3-pentanone (0.50 mL, 5.0 mmol) in 50 mL of dry THF was added in one portion, and heating was continued at reflux for 6 h. Then the reaction mixture was cooled to rt, quenched with 10% aqueous K_2CO_3 (100 mL) and extracted with ethyl acetate (3 × 80 mL). The combined organic phase was washed with brine (50 mL), dried over Na_2SO_4, and evaporated to give a residue, which was flash column-chromatographed (3:1 hexane/ethyl acetate) to afford **1** (383.4 mg, 88.3%) as a white solid.

1: Mp. 76.0–76.5 °C (colorless needles, recrystallized from *n*-hexane). ^{1}H NMR ($CDCl_3$) δ: 7.261 (2H, t, J = 8.0 Hz), 7.173 (1H, d, J = 7.2 Hz), 7.128 (2H, d, J = 7.6 Hz), 7.009 (2H, d, J = 8.8 Hz), 6.726 (2H, d, J = 8.8 Hz), 4.763 (1H, s), 2.152 (2H, quartet, J = 7.6 Hz), 2.115 (2H, quartet, J = 6.0 Hz), 1.007 (3H, t, J = 7.6 Hz), 0.994 (3H, t, J = 7.6 Hz). ^{13}C NMR ($CDCl_3$) δ: 153.7, 143.7, 142.0, 136.5, 136.2, 130.5, 129.2, 127.9, 125.9, 114.8, 24.4, 24.3, 13.3. HRMS (ESI^-, $[M - H]^-$): Calcd. for $C_{18}H_{19}O^-$, 251.14414. Found: 251.14730. HRMS (FAB-MS, $[M]^+$) Calcd. for $C_{18}H_{20}O$, 252.1514. Found: 252.1528. Anal. Calcd. for $C_{18}H_{20}O$: C, 85.67; H, 7.99; N, 0.00. Found: C, 85.38; H, 8.13; N, 0.00.

*Compound **4** (YAK06).*

2-Dimethylaminoethyl chloride hydrochloride (282.4 mg, 2.0 mmol) and K_2CO_3 (1.5734 g, 11.4 mmol) were stirred in acetone/H_2O (18 mL/2 mL) at 0 °C for 30 min, then compound **1** (139.1 mg, 0.55 mmol) and K_2CO_3 (421.1 mg, 3.1 mmol) were added, and the whole was heated at reflux for 24 h, then cooled to rt. Inorganic materials were removed by filtration, and the filtrate was evaporated. The residue was flash column-chromatographed (100:1 ethyl acetate/Et_3N) to afford the amine as a white solid (88.0 mg). To a solution of the amine in ethyl acetate, a solution of HCl in ether was added to give a precipitate, which was collected and recrystallized from ethanol/ethyl acetate to give **4** (95.0 mg, 48%) as a white powder. **4**: Mp. 129.5–130.2 °C. ^{1}H NMR ($CDCl_3$) δ 726–6.90 (9H, m), 4.07 (2H, t, J = 6.0 Hz), 2.75 (2H, t, J = 6.0 Hz), 2.40 (6H, s), 2.15 (4H, d, J = 7.2 Hz), 1.00 (6H, t, J = 7.2 Hz). HRMS (FAB-MS, $[M\text{-}Cl]^+$): Calcd. for $C_{22}H_{30}NO^+$: 324.2322. Found: 324.2321.

dx.doi.org/10.1021/cn200091w | *ACS Chem. Neurosci.* 2012, 3, 105–113

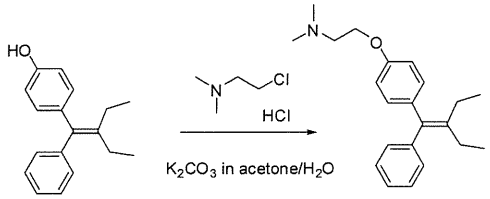

1 (YAK01)

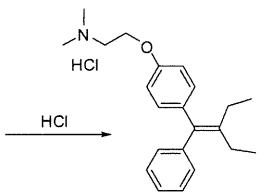

4 (YAK06)

Biology. All procedures using live animals in this study were conducted in accordance with the guidelines of the National Institute of Health Sciences, Japan.

Materials. Dulbecco's modified Eagle's medium (DMEM) and fetal bovine serum (FBS) were purchased from GIBCO (CA, USA). Glutamate dehydrogenase (GLD) was purchased from Roche (Mannheim, Germany). β-Nicotinamide adenine dinucleotide (βNAD), 3-(4,5-dimethyl-2-thiazolyl)-2,5-diphenyl-2H-tetrazolium bromide (MTT), 1-methoxy-5-methylphenazinium methyl sulfate (MPMS), lactate lithium salt and LY294002 were purchased from Sigma (MO, USA). DL-threo-β-benzyloxyaspartic acid (TBOA) and ICI182,780 were purchased from Tocris (MO, USA). U0126 was purchased from Promega (WI, USA). Assay kits for hormonal effects on HEK293/hERα and HEK293/hERβ reporter cells were purchased from Clontech (CA, USA).

Cell Culture. Primary cultures of astrocytes were prepared from the cerebral cortices of 3-day-old neonates of Wistar rats, as described previously.[31] Briefly, dissociated cortical cells were suspended in modified DMEM containing 30 mM glucose, 2 mM glutamine, 1 mM pyruvate and 10% FBS, and plated on uncoated 75 cm^2 flasks at the density of 600 000 cells/cm^2. A monolayer of type I astrocytes was obtained 12–14 days after plating. Nonastrocytes such as microglia were detached from the flasks by shaking and removed by changing the medium. Astrocytes in the flasks were dissociated by trypsinization, reseeded on uncoated 96-well microtiter plates at 20 000 cells/cm^2, and incubated until the cells became confluent (approximately 9–10 days after reseeding). In this culture, >98% of the cells were identified as type I astrocytes on the basis of positivity for GFAP and flattened, polygonal appearance.

Measurement of Extracellular L-Glu Concentration. Extracellular L-Glu concentration was measured by means of a colorimetric method according to Abe et al.[32] Briefly, 50 μL of culture supernatant was transferred to each well of a 96-well microtiter plate and mixed with 50 μL of substrate mixture consisting of 20 U/mL GLD, 2.5 mg/mL β-NAD, 0.25 mg/mL MTT, 100 μM MPMS and 0.1% (v/v) Triton X-100 in 0.2 M Tris-HCl buffer (pH 8.2). After 10 min incubation at 37 °C, the reaction was stopped by adding 100 μL of solution containing 50% (v/v) dimethylformamide and 20% (wt/vol) SDS (pH 4.7). In this reaction, MTT (yellow) is converted into MTT formazan (purple) in proportion to the L-Glu concentration. The amount of MTT formazan was determined by measuring the absorbance at 570 nm (test wavelength) and 655 nm (reference wavelength) with a microplate reader. The concentration of L-Glu was estimated from a standard curve, which was constructed in each assay using cell-free medium containing known concentrations of L-Glu. L-Glu clearance was shown as the amount of L-Glu taken up by astrocytes, which was calculated from the concentration difference in the medium.

Treatment with Test Compounds. L-Glu was dissolved at 1 mM in phosphate-buffered saline and diluted to 100 μM with the culture medium. Compounds **1**, **2**, **3**, and **4** were dissolved at 100, 100, 100, and 10 mM, respectively, in dimethyl sulfoxide (DMSO) and diluted to the required final concentrations with the culture medium. The concentration of DMSO in the medium was controlled to be below 0.1%, because we had already confirmed that 0.1% DMSO has no effect on L-Glu transport activity or cell viability (data not shown). Cells were incubated with test compounds for 24 h. TBOA (IC50 = 48 μM for GLAST, 7 μM for GLT1) was freshly dissolved at 1 mM in culture medium for each experiment. ICI182,780 (IC50 = 0.29 nM for ERs), U0126 (IC50 = 72 nM for MEK1, 58 nM for MEK2), and LY294002 (IC50 = 1 μM for class 1 PI3K, 19 μM for class 2 PI3K) were dissolved at 1, 5, and 5 mM, respectively, in DMSO, and the solutions were diluted with culture medium to yield the required final concentrations. These inhibitors were coapplied with 1 nM test compounds (**1**–**4**) for 24 h.

Assay Procedure for Hormonal Effects on HEK293/hERα and HEK293/hERβ Reporter Cells. Human embryo kidney 293 cells (HEK293) were grown in FBS (+) DMEM in 100 mm dishes. Cells were subcultured once or twice a week at about 80% confluence. A solution of 12.4 μL of 2 M calcium ion, 100 ng/well reporter or negative control vector (pERE-TA-SEAP or pTA-SEAP, Clontech), 50 ng/well expression vector (pcDNA3 ERα or pcDNA3 ERβ, generous gift from Dr. Shige-aki Kato, University of Tokyo, Japan), and 100 ng/well positive control vector (pSV-β-galactosidase, Promega) was diluted to a final volume of 10 μL/well. This mixture was carefully added dropwise to the same volume of HEPES solution with slow vortexing, and the mixture was incubated at rt for 20 min to obtain a precipitate. Cells from the exponential growth phase were seeded (3.0×10^4 cells/ml) into 96-well plates the day before transfection. The cells were incubated with fresh medium for 1 h, then 1/10 volume of precipitate was added to each well and incubation was continued for 24 h at 37 °C in an atmosphere of 5% CO_2 in air. The medium was replaced with fresh FBS (-) medium and incubation was continued for a further 24 h. Then the cells were incubated with test compounds for 24 h at 37 °C in an atmosphere of 5% CO_2 in air. SEAP activity (Great EscapeTM SEAP chemiluminescence kit 2.0, Clontech) and β-galactosidase activity (β-Galactosidase Enzyme Assay System with Reporter Lysis Buffer, Promega) were measured with a Spectramax M5 microplate reader (Molecular Devices Japan, Tokyo, Japan). All transfections were performed in triplicate.

Statistical Analysis. Data were obtained from four independent experiments (averaged values of six wells for each) unless otherwise noted. Data are expressed as means ± SEM of these data. Tests of homogeneity of variance, normality, and distribution were performed to ensure that the assumptions required for standard parametric ANOVA were satisfied. Statistical analysis was performed by one-way repeated-measures ANOVA with post hoc Tukey's test for multiple pairwise comparisons.

AUTHOR INFORMATION

Corresponding Author

*(K.S.) Telephone and Fax: +81-3-3700-9698. E-mail: kasato@nihs.go.jp. (T.O.) Telephone: +81-3-5840-4730. Fax: +81-3-5840-4735. E-mail: ohwada@mol.f.u-tokyo.ac.jp.

Author Contributions

†These two authors equally contributed to this Article. Individual author contributions: K.S. designed the biological experimental plan, performed biological experiments, data analysis, manuscript writing and preparation. J.K. and Y.S. performed experimental work. K.T. contributed to the data analysis. J.O., K.N. and Y.S. provided advice on the experimental direction. Y.O. carried out organic synthesis, data analysis and wrote portions of the manuscript. Y.S. carried out organic synthesis. T.O. designed and oversaw all organic chemistry studies, carried out organic synthesis and also performed data analysis and manuscript writing and preparation.

Funding

This work was partly supported by a Grant-in-Aid from the Food Safety Commission, Japan (No. 1003), a Grant-in-Aid for Young Scientists from MEXT, Japan (KAKENHI 21700422), the Program for Promotion of Fundamental Studies in Health Sciences of NIBIO, Japan, a Health and Labor Science Research Grant for Research on Risks of Chemicals, a Health and Labor Science Research Grant for Research on New Drug Development from MHLW, Japan, awarded to K.S., and a Health and Labor Science Research Grant for Research on Risks of Chemicals from MHLW, Japan, awarded to K.N. and T.O.

Notes

The authors declare no competing financial interest.

■ ACKNOWLEDGMENTS

We thank Dr. Shige-aki Kato for providing pcDNA3 hERα and pcDNA3 hERβ.

■ ABBREVIATIONS

βNAD; β-nicotinamide adenine dinucleotide; CNS; central nervous system; DMEM; Dulbecco's modified Eagle's medium; DMSO; dimethyl sulfoxide; E2; 17β-estradiol; ESI; electron spray ionization; FBS; fetal bovine serum; GLD; glutamate dehydrogenase; HEK-293; Human embryo kidney 293 cells; HRMS; high-resolution mass spectrometry; L-Glu; L-glutamate; MAPK; mitogen-activated protein kinase; MEK; mitogen-activated protein kinase/extracellular signal-regulated kinase; mERα; membrane-associated estrogen receptor α; mGluR5; metabotropic glutamate receptor 5; MPMS; 1-methoxy-5-methylphenazinium methyl sulfate; MTT; 3-(4,5-dimethyl-2-thiazolyl)-2,5-diphenyl-2H-tetrazolium bromide; nERs; nuclear estrogen receptors; PI3K; phosphatidylinositol 3-kinase; Tam; tamoxifen; TBOA; DL-threo-β-benzyloxyaspartic acid; TLC; thin-layer chromatography; TOF; time-of-flight

■ REFERENCES

(1) Kumar, A., Singh, R. L., and Babu, G. N. (2010) Cell death mechanisms in the early stages of acute glutamate neurotoxicity. *Neurosci. Res. 66*, 271–278.

(2) Choi, D. W. (1988) Glutamate neurotoxicity and diseases of the nervous system. *Neuron 1*, 623–634.

(3) Logan, W. J., and Snyder, S. H. (1971) Unique high affinity uptake systems for glycine, glutamic and aspartic acids in central nervous tissue of the rat. *Nature 234*, 297–299.

(4) Beart, P. M., and O'Shea, R. D. (2007) Transporters for L-glutamate: an update on their molecular pharmacology and pathological involvement. *Br. J. Pharmacol. 150*, 5–17.

(5) Sato, K., Matsuki, N., Ohno, Y., and Nakazawa, K. (2003) Estrogens inhibit L-glutamate uptake activity of astrocytes via membrane estrogen receptor alpha. *J. Neurochem. 86*, 1498–1505.

(6) Olivier, S., Close, P., Castermans, E., de Leval, L., Tabruyn, S., Chariot, A., Malaise, M., Merville, M. P., Bours, V., and Franchimont, N. (2006) Raloxifene-induced myeloma cell apoptosis: a study of nuclear factor-kappaB inhibition and gene expression signature. *Mol. Pharmacol. 69*, 1615–1623.

(7) Sato, K., Saito, Y., Oka, J., Ohwada, T., and Nakazawa, K. (2008) Effects of tamoxifen on L-glutamate transporters of astrocytes. *J. Pharmacol. Sci. 107*, 226–230.

(8) Bunch, L., Erichsen, M. N., and Jensen, A. A. (2009) Excitatory amino acid transporters as potential drug targets. *Expert Opin. Ther. Targets 13*, 719–731.

(9) Margueron, R., Duong, V., Bonnet, S., Escande, A., Vignon, F., Balaguer, P., and Cavailles, V. (2004) Histone deacetylase inhibition and estrogen receptor alpha levels modulate the transcriptional activity of partial antiestrogens. *J. Mol. Endocrinol. 32*, 583–594.

(10) Thompson, D. S., Spanier, C. A., and Vogel, V. G. (1999) The relationship between tamoxifen, estrogen, and depressive symptoms. *Breast J. 5*, 375–382.

(11) Grilli, S. (2006) Tamoxifen (TAM): the dispute goes on. *Ann. Ist. Super. Sanita 42*, 170–173.

(12) Sha, Y., Tashima, T., Mochizuki, Y., Toriumi, Y., Adachi-Akahane, S., Nonomura, T., Cheng, M., and Ohwada, T. (2005) Compounds structurally related to tamoxifen as openers of large-conductance calcium-activated K^+ channel. *Chem. Pharm. Bull. (Tokyo) 53*, 1372–1373.

(13) Robertson, D. W., Katzenellenbogen, J. A., Long, D. J., Rorke, E. A., and Katzenellenbogen, B. S. (1982) Tamoxifen antiestrogens. A comparison of the activity, pharmacokinetics, and metabolic activation of the cis and trans isomers of tamoxifen. *J. Steroid Biochem. 16*, 1–13.

(14) Weltje, L., vom Saal, F. S., and Oehlmann, J. (2005) Reproductive stimulation by low doses of xenoestrogens contrasts with the view of hormesis as an adaptive response. *Hum. Exp. Toxicol. 24* (9), 431–437.

(15) Perego, C., Vanoni, C., Bossi, M., Massari, S., Basudev, H., Longhi, R., and Pietrini, G. (2000) The GLT-1 and GLAST glutamate transporters are expressed on morphologically distinct astrocytes and regulated by neuronal activity in primary hippocampal co-cultures. *J. Neurochem. 75*, 1076–1084.

(16) Guillet, B., Lortet, S., Masmejean, F., Samuel, D., Nieoullon, A., and Pisano, P. (2002) Developmental expression and activity of high affinity glutamate transporters in rat cortical primary cultures. *Neurochem. Int. 40*, 661–671.

(17) Razandi, M., Pedram, A., Greene, G. L., and Levin, E. R. (1999) Cell membrane and nuclear estrogen receptors (ERs) originate from a single transcript: studies of ERalpha and ERbeta expressed in Chinese hamster ovary cells. *Mol. Endocrinol. 13*, 307–319.

(18) Pappas, T. C., Gametchu, B., and Watson, C. S. (1995) Membrane estrogen receptors identified by multiple antibody labeling and impeded-ligand binding. *FASEB J. 9*, 404–410.

(19) Grove-Strawser, D., Boulware, M. I., and Mermelstein, P. G. (2010) Membrane estrogen receptors activate the metabotropic glutamate receptors mGluR5 and mGluR3 to bidirectionally regulate CREB phosphorylation in female rat striatal neurons. *Neuroscience 170*, 1045–1055.

(20) Mannella, P., and Brinton, R. D. (2006) Estrogen receptor protein interaction with phosphatidylinositol 3-kinase leads to activation of phosphorylated Akt and extracellular signal-regulated kinase 1/2 in the same population of cortical neurons: a unified mechanism of estrogen action. *J. Neurosci. 26*, 9439–9447.

(21) Szego, E. M., Barabas, K., Balog, J., Szilagyi, N., Korach, K. S., Juhasz, G., and Abraham, I. M. (2006) Estrogen induces estrogen receptor alpha-dependent cAMP response element-binding protein phosphorylation via mitogen activated protein kinase pathway in basal forebrain cholinergic neurons in vivo. *J. Neurosci. 26*, 4104–4110.

(22) Vasudevan, N., Kow, L. M., and Pfaff, D. (2005) Integration of steroid hormone initiated membrane action to genomic function in the brain. *Steroids 70*, 388–396.

(23) Alyea, R. A., Laurence, S. E., Kim, S. H., Katzenellenbogen, B. S., Katzenellenbogen, J. A., and Watson, C. S. (2008) The roles of membrane estrogen receptor subtypes in modulating dopamine transporters in PC-12 cells. *J. Neurochem. 106* (4), 1525–1533.

(24) Watson, C. S., Alyea, R. A., Hawkins, B. E., Thomas, M. L., Cunningham, K. A., and Jakubas, A. A. (2006) Estradiol effects on the dopamine transporter - protein levels, subcellular location, and function. *J. Mol. Signaling 1*, 5.

(25) Filardo, E. J., and Thomas, P. (2005) GPR30: a seven-transmembrane-spanning estrogen receptor that triggers EGF release. *Trends. Endocrinol. Metab. 16* (8), 362–367.

(26) Revankar, C. M., Cimino, D. F., Sklar, L. A., Arterburn, J. B., and Prossnitz, E. R. (2005) A transmembrane intracellular estrogen receptor mediates rapid cell signaling. *Science 11;307* (5715), 1625–1630.

(27) Filardo, E. J., Quinn, J. A., Bland, K. I., and Frackelton, A. R. Jr. (2000) Estrogen-induced activation of Erk-1 and Erk-2 requires the G

protein-coupled receptor homolog, GPR30, and occurs via transactivation of the epidermal growth factor receptor through release of HB-EGF. *Mol. Endocrinol. 14* (10), 1649–1660.
(28) Thomas, P., Pang, Y., Filardo, E. J., and Dong, J. (2005) Identity of an estrogen membrane receptor coupled to a G protein in human breast cancer cells. *Endocrinology 146* (2), 624–632.
(29) Kuo, J., Hamid, N., Bondar, G., Prossnitz, E. R., and Micevych, P. (2010) Membrane estrogen receptors stimulate intracellular calcium release and progesterone synthesis in hypothalamic astrocytes. *J. Neurosci. 30* (39), 12950–12957.
(30) Kisanga, E. R., Gjerde, J., Guerrieri-Gonzaga, A., Pigatto, F., Pesci-Feltri, A., Robertson, C., Serrano, D., Pelosi, G., Decensi, A., and Lien, E. A. (2004) Tamoxifen and metabolite concentrations in serum and breast cancer tissue during three dose regimens in a randomized preoperative trial. *Clin. Cancer Res. 10*, 2336–2343.
(31) Suzuki, K., Ikegaya, Y., Matsuura, S., Kanai, Y., Endou, H., and Matsuki, N. (2001) Transient upregulation of the glial L-glutamate transporter GLAST in response to fibroblast growth factor, insulin-like growth factor and epidermal growth factor in cultured astrocytes. *J. Cell Sci. 114*, 3717–3725.
(32) Abe, K., Abe, Y., and Saito, H. (2000) Evaluation of L-glutamate clearance capacity of cultured rat cortical astrocytes. *Biol. Pharm. Bull. 23*, 204–207.

Cell Mol Neurobiol
DOI 10.1007/s10571-012-9829-z

SHORT COMMUNICATION

Cell-Autonomous Enhancement of Glutamate-Uptake by Female Astrocytes

Yosuke Morizawa · Kaoru Sato · Junpei Takaki · Asami Kawasaki · Keisuke Shibata · Takeshi Suzuki · Shigeru Ohta · Schuichi Koizumi

Received: 27 February 2012 / Accepted: 8 March 2012

Abstract Since gonadal female hormones act on and protect neurons, it is well known that the female brain is less vulnerable to stroke or other brain insults than the male brain. Although glial functions have been shown to affect the vulnerability of the brain, little is known if such a sex difference exists in glia, much less the mechanism that might cause gender-dependent differences in glial functions. In this study, we show that in vitro astrocytes obtained from either female or male pups show a gonadal hormone-independent phenotype that could explain the gender-dependent vulnerability of the brain. Female spinal astrocytes cleared more glutamate by GLAST than male ones. In addition, motoneurons seeded on female spinal astrocytes were less vulnerable to glutamate than those seeded on male ones. It is suggested that female astrocytes uptake more glutamate and reveal a stronger neuroprotective effect against glutamate than male ones. It should be noted that such an effect was independent of gonadal female hormones, suggesting that astrocytes have cell-autonomous regulatory mechanisms by which they transform themselves into appropriate phenotypes.

Keywords Astrocytes · Sex difference · GLAST · Glutamate · Neurotoxicity

Y. Morizawa · K. Shibata · S. Koizumi (✉)
Department of Neuropharmacology, Graduate School of Medicine and Engineering, University of Yamanashi, Yamanashi, Japan
e-mail: skoizumi@yamanashi.ac.jp

Y. Morizawa · S. Ohta
Graduate School of Biomedical Sciences, Hiroshima University, Hiroshima, Japan

K. Sato · J. Takaki
Division of Pharmacology, National Institute of Health Sciences, Tokyo, Japan

J. Takaki · T. Suzuki
Division of Basic Biological Sciences, Keio University, Tokyo, Japan

A. Kawasaki
Center for Trans-Disciplinary Research, Niigata University, Niigata, Japan

Introduction

Astrocytes control synaptic transmission by releasing gliotransmitters such as ATP and glutamate or by uptaking excess neurotransmitters (Haydon 2001; Koizumi et al. 2003). As for the clearance of neurotransmitters, astrocytes express excitatory amino acid transporter 1 (EAAT1; GLAST) or EAAT2 (GLT-1), by which they control the extracellular glutamate concentrations and excitatory neurotransmission. Thus, the functions of these transporters are highly involved in glutamate-dependent excitotoxicity or various neuronal diseases.

It is well known clinically and experimentally that female brain is more resistant to various brain insults or neurodegenerative diseases than male brain, and such sex differences have been historically attributed to the protective effect of gonadal female hormones such as estrogen. Studies by Sato et al. (2003) and Pawlak et al. (2005) have already shown that, exogenously applied 17β-estradiol (E2), the most potent mammalian estrogen, affects the activity of glutamate uptake in astrocytes, which may in part explain the gender difference in brain vulnerability. However, sexual dimorphism generally persists well beyond menopause (Sacco et al. 1998), suggesting that sex differences in brain injury may not be entirely related to the

Published online: 27 March 2012